

Thermal strain analysis of an electronics package using the SEM Moiré technique

Z.W. Zhong

Nanyang Technological University, Singapore

S.K. Nah

Nanyang Technological University, Singapore

Keywords

Strain measurement,
Mathematical analysis,
Electrical components

Abstract

This paper reports on a study of the scanning electron microscope (SEM) Moiré method. Tests were carried out by rotating the specimen grating slightly with respect to the electron scanning raster lines, to verify that the Moiré images captured were really due to the interference between specimen and reference gratings. The experimental results coincided well with the calculated theoretical values and with small measurement errors. Then, the shear strains experienced by the solder joints of a flip-chip ball grid array specimen were investigated using the SEM Moiré method. The results were compared with those obtained using the optical Moiré method.

Introduction

In electronics packages, the thermal mismatch between materials, such as the silicon chip and the substrate used, can cause interconnections to fatigue during operation (Harper, 1997). The mismatch may also cause mechanical and/or electrical failures of the packages (Lau, 1995). Optical Moiré interferometry has previously been used to analyse the thermal deformations and strains of electronics packages by Han and Guo (1995), Han and Post (1992) and Zhong *et al.* (2001).

The objective of this study was to investigate the thermal deformations of an electronics package using the scanning electron microscope (SEM) Moiré method and compare the results with those obtained from the optical Moiré method. The specimen used to obtain Moiré fringes in order to evaluate the thermal deformations was a flip-chip ball grid array (FCBGA) package. A holographic uniform cross-line grating was replicated onto the cross-sectioned surface of the FCBGA package at 100°C and then cooled to room temperature (25°C). Under a SEM, the holographic grating (specimen grating) and the electron beam scan (reference grating) interfered and formed SEM Moiré patterns. With the SEM Moiré fringes obtained, the shear strains in different solder joints were analysed. The results of the shear strains were then compared with the previously measured results obtained using the optical Moiré interferometry technique.

The SEM Moiré technique and strain analysis

Traditionally, Moiré interferometry is an optical experimental technique and provides high sensitivity deformation measurement (Dally and Riley, 1994; Guild, 1956; Sciammarella, 1982). Optical Moiré fringes are widely employed in experimental mechanics (Graham and Sanford, 1988; Post *et al.*, 1994; Theocaris, 1969; Zhong *et al.*, 2002).

The SEM Moiré method is a novel technique compared to the traditional Moiré methods. When a specimen surface that carries a regular array of lines is examined under a SEM, Moiré fringes can be observed. The difference between the optical Moiré and SEM Moiré is that in the latter, no actual reference grating exists. Instead, the electron-beam raster scan replaces the reference grating (Dally and Read, 1993; Read and Dally, 1996).

Rotation of the SEM Moiré fringes occurs when the pitches of the specimen grating and the electron-beam raster scan (reference grating) are closely matched and one grating is rotated, with the other grating being fixed. The Moiré fringes should rotate following the relationship

expressed by the following equation (Read and Dally, 1996; Zhong *et al.*, 2000).

$$\frac{\sin(\phi - \theta)}{\sin \phi} = \frac{P_s}{P_r} = C \quad (1)$$

where C is a constant; ϕ and θ are the Moiré fringe rotation angle and the specimen grating rotation angle with respect to the reference grating, i.e. the electron-beam raster scan-lines, respectively; and P_s and P_r are the pitch values of the specimen grating and the electron-beam raster scan-lines (the reference grating), respectively.

When a cross-line specimen grating is utilised, the U -field (displacement in the x direction) and V -field (displacement in the y direction) SEM Moiré fringes can be separately generated by adjusting the orientation of the specimen grating parallel or perpendicular to the grating lines of the reference grating. Using the Moiré patterns corresponding to the U and V fields, the strain components ϵ_x , ϵ_y , and γ_{xy} in the x - y plane can be analysed by using the following equations (Zhong *et al.*, 2000).

$$\epsilon_x = \frac{P_s}{S_{xx}^1} - \frac{P_s}{S_{xx}^0} \quad (2)$$

$$\epsilon_y = \frac{P_s}{S_{yy}^1} - \frac{P_s}{S_{yy}^0} \quad (3)$$

$$\gamma_{xy} = \frac{P_s}{S_{xy}^1} + \frac{P_s}{S_{yx}^1} - \frac{P_s}{S_{xy}^0} - \frac{P_s}{S_{yx}^0} \quad (4)$$

where S_{xx}^0 and S_{yy}^0 are the spacing values between the two adjacent fringes in the initial U -field and V -field Moiré patterns before deformation, respectively. S_{xx}^1 and S_{yy}^1 are the spacing values between two adjacent U -field and V -field Moiré fringes in x and y directions after deformation, respectively. S_{xy}^0 is the spacing between the adjacent U -field Moiré fringes in the y direction before deformation, S_{yx}^0 is the spacing between the adjacent V -field Moiré fringes in the x direction before deformation, and S_{xy}^1 and S_{yx}^1 are the spacing values between the adjacent U - and V -field Moiré fringes in the y and x directions after deformation, respectively.

Formation of SEM Moiré fringes on the diffraction grating

The specimen diffraction grating used in this study had 1,200 lines/mm, i.e. $P_s = 833$ nm. A SEM was used to observe the diffraction grating at high magnifications. The SEM scan line pitch was set to 1,280 lines/mm, i.e. $P_r = 781$ nm. Figure 1 shows a SEM image of the diffraction grating at a magnification of 11,000.

Received: 7 May 2003
Revised: 21 July 2003
Accepted: 28 July 2003



Soldering & Surface Mount
Technology
15/3 [2003] 33–35

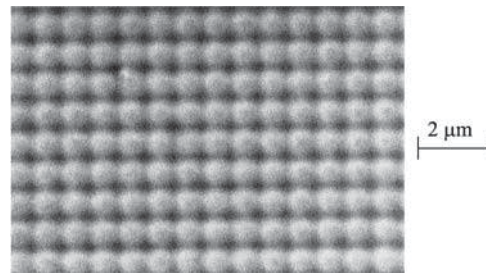
© MCB UP Limited
[ISSN 0954-0911]
[DOI: 10.1108/09540910310505107]

The Emerald Research Register for this journal is available at
<http://www.emeraldinsight.com/researchregister>



The current issue and full text archive of this journal is available at
<http://www.emeraldinsight.com/0954-0911.htm>

Figure 1
 SEM image of the diffraction grating



The SEM beam was scanned such that information was collected in a raster pattern. The scan lines formed the reference grating while the diffraction grating was the specimen grating. Figure 2 schematically shows the raster pattern of the SEM scanner. SEM Moiré images were created by the overlapping of the two gratings, and appeared on the screen of the SEM monitor. The images were recorded for analysis.

Effect of rotational angle on SEM Moiré fringes

When a specimen grating is rotated in a SEM, there is a difference in angle between the electron scanning raster lines and the specimen grating. This also causes rotation of the SEM Moiré fringes. Tests were carried out by rotating the specimen grating slightly with respect to the electron scanning raster lines, to verify that the Moiré images captured were really formed by the interference between the specimen grating and reference grating.

The specimen grating in the SEM was aligned so that the grating lines were parallel to the scanning lines. The specimen grating was rotated so that the angle θ changed from -2° to 2° in steps of 0.5° . Upon varying the values of θ , the corresponding images of the Moiré fringes were captured and their rotation angles (ϕ) were measured. Figure 3 shows the SEM Moiré fringe patterns at $\theta = -2^\circ, 0, 2^\circ$. Table I shows the measured ϕ values.

Using equation (1), ϕ values were calculated and are shown in Table I. The experimental results coincided well with the calculated theoretical values with small measurement errors.

Strain analysis of a FCBGA package

After it was confirmed that the fringes obtained were real SEM Moiré fringes formed by the specimen and reference gratings, the SEM Moiré method was applied to strain analysis of an electronics package.

The test specimen used for this strain measurement was a FCBGA package mounted on a bismaleimide triazine (BT) substrate. The FCBGA sample had several rows of peripheral solder joints. The dimensions of these solder joints are diameter = 0.3 mm, height = 0.2 mm, and

Figure 2
 Raster scanning pattern of the electron beam

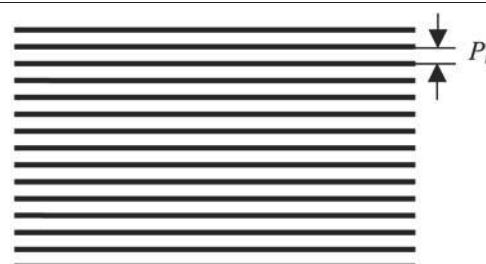
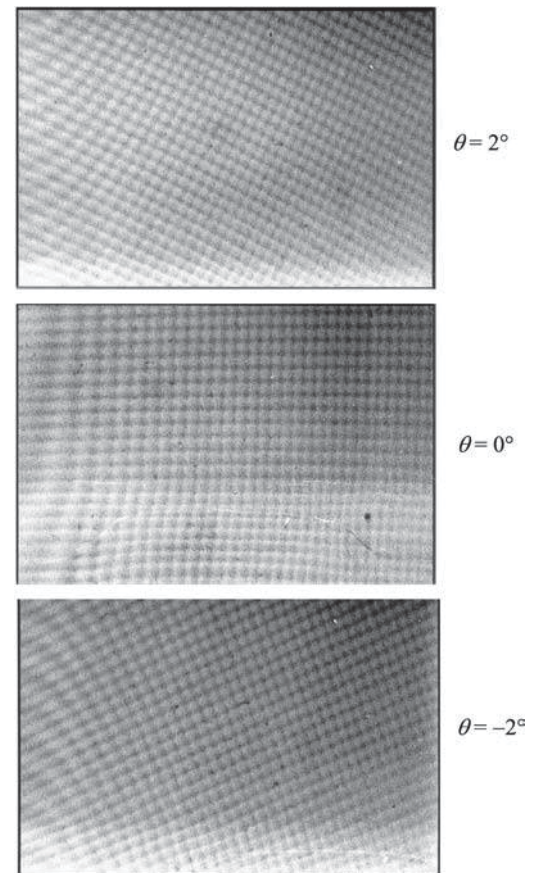


Figure 3
 Moiré fringe patterns at various rotation angles



pitch = 0.75 mm. The chip had dimensions of $10.3 \times 10.3 \times 0.67$ mm and the BT substrate had dimensions of $38 \times 26 \times 0.5$ mm. The specimen was cross-sectioned to expose the solder joints. A holographic uniform cross-line grating (1,200 lines/mm) was replicated onto the cross-sectioned surface of the FCBGA package using a special adhesive. The grating could withstand a temperature of less than 120°C . Therefore, the grating replication was performed at 100°C . After the transfer of the grating, the sample was then cooled to room temperature (25°C), because the strain analysis was conducted at room temperature. The thermal deformation of the specimen caused by the temperature change of -75°C (i.e. from 100 to 25°C) was recorded by the deformed specimen grating (Zhong *et al.*, 2001).

The package with the deformed specimen grating was carefully mounted on the SEM stage using a conductive adhesive to allow the analysis of the thermal deformation using the SEM Moiré method. Under the SEM, the deformed holographic grating (specimen grating) and the electron

Table I
 The calculated and measured values of the Moiré fringe rotation angles

θ ($^\circ$)	Measured ϕ ($^\circ$)	Calculated ϕ ($^\circ$)
2	-28	-27.3
1.5	-21	-21.2
1	-14	-14.6
0.5	-7	-7.4
0	0	0
-0.5	6	7.4
-1	15	14.6
-1.5	21	21.2
-2	26	27.3

beam scan (reference grating) interfered and formed SEM Moiré patterns. These Moiré fringes were used to calculate the strains in the solder joints using equations (2)-(4).

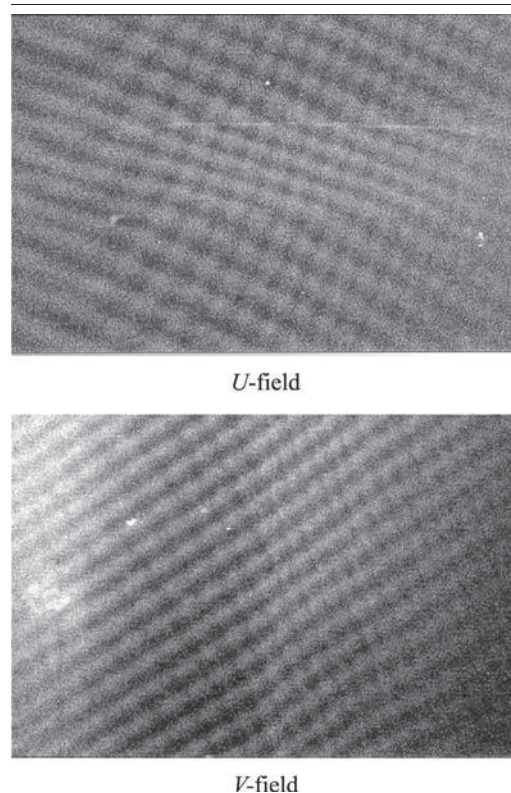
The subject areas for the study were the solder joints from the corner to the centre of the chip. The joints in one half of the cross-section were observed and both the *U*-field and the *V*-field Moiré images were captured. Examples of the Moiré patterns observed in the solder joints are shown in Figure 4.

Using the Moiré patterns corresponding to the *U*- and *V*-fields, the shear strains could be calculated. Figure 5 shows

the shear strain values for the solder joints. The figure also compares the shear strain values with the values obtained from previous work using optical Moiré interferometry (Zhong *et al.*, 2001).

The FCBGA package consisted of different materials with different thermal expansion coefficients. Therefore, inhomogeneous thermal strain occurred when the package underwent a temperature change of -75°C from 100°C to 25°C . The measurement results show that the values of the shear strain varied between the different solder joints. The shear strain caused by the thermal loading decreased sharply with increasing distance away from the corner of the die, i.e. the corner solder joint experienced the highest strain, and the joint nearest to the centre experienced the least strain.

Figure 4
 Examples of SEM Moiré fringe patterns



Conclusions

The SEM Moiré technique can be a useful method for deformation study of a wide range of problems in deformation analysis. In this study, the SEM Moiré technique has been successfully applied to the strain analysis of an electronics package. Deformation measurement with a high resolution is possible by using the SEM Moiré technique. Further study is being carried out.

The SEM Moiré technique was used to determine the shear strains in an electronics package in this study. The interference pattern was formed by grating replication on a specimen and bombarding the grating specimen with electron beams. The thermal shear strains in the solder joints were calculated using the Moiré patterns observed with a SEM. The results were compared with those obtained using the optical Moiré method and they coincided well.

References

- Dally, J.W. and Read, D.T. (1993), "Electron beam Moiré", *Experimental Mechanics*, Vol. 33, pp. 270-7.
- Dally, J.W. and Riley, W.F. (1994), *Experimental Stress Analysis*, 3rd ed., McGraw-Hill, New York.
- Graham, S.M. and Sanford, R.J. (1988), "The influence of grating characteristics on Moiré fringe multiplication", *Experimental Mechanics*, Vol. 28, pp. 329-35.
- Guilid, J. (1956), *The Interference Systems of Crossed Diffraction Gratings, Theory of Moiré Fringes*, Oxford University Press, New York.
- Han, B. and Guo, Y. (1995), "Thermal deformation analysis of various electronic packaging products by Moiré and microscope Moiré interferometry", *Journal of Electronic Packages, Transaction of ASME*, Vol. 117 No. 3, pp. 185-91.
- Han, B. and Post, D. (1992), "Immersion interferometer for microscopic Moiré interferometry", *Experimental Mechanics*, Vol. 31 No. 1, pp. 38-41.
- Harper, C.A. (1997), *Electronic Packaging and Interconnection Handbook*, McGraw-Hill, New York.
- Lau, J.H. (1995), *Flip Chip Technologies*, McGraw-Hill, New York.
- Post, D., Han, B. and Ifju, P. (1994), *High Sensitivity Moiré: Experimental Analysis for Mechanics and Materials*, Springer-Verlag, New York.
- Read, D.T. and Dally, J.W. (1996), "Theory of electron beam Moiré", *Journal of Research National Institute of Standards and Technology*, Vol. 101, pp. 47-61.
- Sciammarella, C.A. (1982), "The Moiré method, a review", *Experimental Mechanics*, Vol. 22 No. 11, pp. 418-33.
- Theocaris, P.S. (1969), *Moiré Fringes in Strain Analysis*, Pergamon Press, Oxford, New York.
- Zhong, Z.W., Lim, S.C., Asundi, A.K. and Chai, T.C. (2001), "Micro Moiré for thermal deformation investigation in electronics packaging", *Proceedings of SPIE*, Vol. 4596, pp. 256-60.
- Zhong, Z.W., Lu, Y.G., Xie, H.M., Ngoi, B.K.A., Yu, J., Chai, J.B. and Asundi, A. (2000), "Measurement of thermal deformation of IC packages using the AFM scanning Moiré technique", *Proceedings of SPIE*, Vol. 4229, pp. 133-41.
- Zhong, Z.W., Shi, X.Q., Wong, K.W. and Wang, Z.P. (2002), "Flip chip interfacial behaviour under thermal testing", *Proceedings of 4th Electronics Packaging Technology Conference (EPTC 2002)*, Singapore, pp. 56-9.

Figure 5
 Comparison of shear strains in the solder joints at different positions as measured using the SEM Moiré and the optical Moiré techniques

